Ukrainian Journal of Physical Optics
ISSUE 4
2026

Optical Properties and Upconversion Luminescence of $Bi_{12}SiO_{20}$:Yb,Er Glass

M. Shevchuk [1], V. Adamiv [2], I. Teslyuk [2], S. Malynych [3], V. Kordan [1], M. Rudysh [1], T. Demkiv [1,*], R. Gamernyk [1]

[1] Ivan Franko National University of Lviv, 8 Kyryla i Mefodiya St., 79005 Lviv, Ukraine
[2] O.G. Vlokh Institute of Physical Optics of the Ivan Franko National University of Lviv, 23 Dragomanov St., Lviv, 79005, Ukraine
[3] Hetman Petro Sahaidachnyi National Army Academy, 32 Heroes of Maidan St., 79012 Lviv, Ukraine
* Corresponding author: taras.demkiv@lnu.edu.ua

Received: 20.10.2026

Abstract. In this work, the luminescence of $Bi_{12}SiO_{20}$ glass doped with ytterbium and erbium ions at different concentration ratios has been studied. According to X-ray diffraction data, the glass is amorphous while retaining sillenite-type short-range order. The absorption and luminescence excitation spectra exhibit the bands of $f-f$ transitions of Er^{3+} ions and an intense $^2F_{7/2}\rightarrow{}^2F_{5/2}$ band of Yb^{3+} ions (976.5 nm). The presence of the Yb^{3+} band in the excitation spectrum of the 1540 nm emission is direct evidence of resonant excitation energy transfer from Yb^{3+} to Er^{3+} ions. Under excitation with λ = 980 nm, an intense intracenter emission band of Er^{3+} ions ($^4I_{13/2}\rightarrow{}^4I_{15/2}$ transition) peaking at 1532 nm with a full width at half maximum of 48 nm is observed, together with green (526–552 nm) and red (657–670 nm) upconversion luminescence caused by a two-step $Yb^{3+}\rightarrow Er^{3+}$ energy transfer channel. It has been established that the width of the 1.5 μm band exceeds the values reported for binary Bi_2O_3–SiO_2 glasses and $Bi_4Si_3O_{12}$:Er,Yb crystals, which makes $Bi_{12}SiO_{20}$:Yb,Er glass a promising active medium for broadband C+L-band amplifiers.

Keywords: sillenite $Bi_{12}SiO_{20}$, bismuth glass, erbium, ytterbium, 1.5 μm luminescence, upconversion, optical amplifier
UDC: 535.37, 535.33
DOI: 10.3116/16091833/Ukr.J.Phys.Opt.2026.04193
This work is licensed under the Creative Commons Attribution International

1. Introduction

Developing telecommunications technologies requires extending the transmission capacity of fiber-optic communication links beyond the standard C-band (1530–1565 nm), which is constrained by the 35–40 nm gain bandwidth of erbium-doped fiber amplifiers. This drives the transition to multi-band transmission: recent E+S+C+L-band transmission experiments employed a combination of bismuth-doped, Raman, and erbium-doped amplifiers [1,2]. Another direction is the development of compact amplifiers based on highly doped multicomponent glasses, in which a gain of up to several dB/cm is achieved in active elements only a few centimeters long [3]. For amplifiers based on Er^{3+} ions, the gain bandwidth is determined primarily by the host matrix. The first comparative studies have shown that silicate, phosphate, and fluoride glasses differ substantially in transition cross-sections, emission bandwidth, and the lifetime of the $^4I_{13/2}$ level [4]. Analysis within the Judd–Ofelt theory explains why heavy-metal oxide hosts with a high refractive index and a large intensity parameter Ω_6 simultaneously provide a larger stimulated emission cross-section and a broader, flatter band in the 1.5 μm region [5]. The product $\sigma_{em}\times\Delta\lambda$ is commonly accepted as the figure of merit for a material in wavelength-multiplexing amplifiers.

The physical reason for the broadening of the emission band is the location of Er^{3+} ions in several non-equivalent sites of the host and the associated inhomogeneous Stark splitting of the levels [6].

The first practical implementation of this approach was erbium-doped tellurite fibers, in which laser generation and amplification were achieved [7]. Uniform signal gain in a single fiber over the 1530–1610 nm range was demonstrated [8], with a noise figure comparable to that of silica-based devices [9], and the operating range was extended into the L-band up to 1.6 μm [10]. Bismuth oxide-based glasses proved promising for telecommunications applications. Tanabe et al. showed that the Er^{3+} emission band in the 1.5 μm region in Bi_2O_3–based glasses has a width of about 79 nm, i.e., it is considerably broader than in silicate glass [11], which became the basis for developing Bi_2O_3-based erbium-doped fibers (Bi-EDF) with very high erbium solubility [12]. The spectroscopic parameters and thermal stability of such glasses proved sufficient for fiber drawing [13]. It should be noted that the main limitations of such highly doped media are cooperative upconversion and pair-induced quenching of Er^{3+} ions. Co-doping with La_2O_3 and B_2O_3 reduces erbium clustering [14], but it also leads to power loss in Bi-EDF [15]. The fraction of paired ions in commercial Bi-EDF is estimated at about 6 % [16], and increasing the dopant concentration is accompanied by concentration quenching of luminescence [17]. These processes increase the noise figure of Bi-EDF compared to less heavily doped hosts [18].

The spectral and kinetic properties of Er^{3+} ions in bismuth glasses have been studied in considerable detail. In binary Bi_2O_3–SiO_2 glasses, the refractive index increases from 1.85 to 2.17 as the Bi_2O_3 content increases from 20 to 55 mol.%, and at 35 mol.% Bi_2O_3, $\sigma_{em} \approx 0.74\times10^{-20}$ cm^2 and an emission bandwidth of 42 nm were obtained [19]. The addition of B_2O_3 broadens the band to 65–82 nm [20], and $Ce^{3+}/Yb^{3+}/Er^{3+}$ triply doped bismuth borosilicate glass is characterized by an emission bandwidth of about 80 nm covering the S+C+L bands [21]. For bismuth germanate glasses, a bandwidth of 52–80 nm, $\sigma_{em} \approx 0.75\times10^{-20}$ cm^2, and a positive gain cross-section in the L-band at a population inversion above 30% were obtained [22]. Excitation energy transfer from Yb^{3+} to Er^{3+} ions was studied [23, 24], as were the properties of Er/Yb in lead-bismuth halogermanates ($\sigma_{em} = 0.89\times10^{-20}$ cm^2, bandwidth ≈ 45 nm) [25]. At the same time, the low phonon energy of bismuthates extends the lifetime of the $^4I_{11}/_2$ level to 2.45 ms [26], which must be taken into account under 980 nm excitation. In binary bismuth borate glasses, the bandwidth reaches 76–86 nm [27], and co-doping with Yb^{3+} ions in heavy-metal borate glasses increases σem almost sixfold and provides a flat gain cross-section in the 1460–1640 nm range [28]. The optimization of energy transfer in the Yb/Er system for the C-band in such glasses was carried out in [29], and for the Bi_2O_3–$BaTiO_3$ system a Judd–Ofelt analysis with an assessment of suitability for a fiber amplifier was performed [30]. Note that even in tellurite glasses, replacing part of TeO_2 with Bi_2O_3 lowers the phonon energy and increases the emission intensity in the 1.5 μm region by almost 40% [31], while Er^{3+}-doped bismuth tellurite glasses provide a gain coefficient of 6.17 cm^{-1} [32].

Doping with ytterbium ions is a widely accepted method for efficiently exciting Er^{3+} ions with 980 nm radiation, owing to the broad, intense absorption band of Yb^{3+} ions ($^2F_7/_2 \rightarrow {}^2F_5/_2$ transition) and nearly resonant energy transfer to the $^4I_{11}/_2$ level of the Er^{3+} ion [33]. In phosphate glass, the Yb→Er energy-transfer coefficient (1.1×10^{-16} cm^3/s) exceeds the cooperative upconversion coefficient by two orders of magnitude [34]. For

bismuth borate glass, a dipole–dipole microparameter C_{DA} = 42×10^{-40} cm^6/s and a critical transfer radius of 10.7 Å were determined [35]. The competing anti-Stokes processes – excited-state absorption, energy-transfer upconversion, and cooperative sensitization – are described in detail in the review [36]. Notably, Er^{3+} ions can also efficiently convert ~1.5 μm telecommunication radiation into visible light [37]. In bismuth-containing hosts, the broadband IR luminescence of bismuth active centers must also be considered. This luminescence was first observed in silicate glass [38] and later in germanate glasses with a bandwidth of over 300 nm [39]. Bismuth-doped fiber amplifiers have been developed based on such centers, and Bi/Er co-doping has provided continuous luminescence in the 1.1–1.6 μm range [40] and C+L+U-band fiber amplifiers [41].

Compounds with the sillenite structure $Bi_{12}MO_{20}$ (M = Si, Ge, Ti) are well known as photorefractive and electro-optic materials; however, as hosts for lanthanide ions, they have been studied comparatively little. For Eu^{3+} ions in $Bi_{12}SiO_{20}$ (BSO) and $Bi_{12}GeO_{20}$ (BGO) crystals, a low-symmetry environment of the Bi site was established, and a Judd–Ofelt analysis was performed [42]. Laser generation was observed in $Bi_{12}SiO_{20}$:Nd crystals [43]. Nano-sillenite $Bi_{12}SiO_{20}$ glass-ceramics were obtained in the Bi_2O_3–ZnO–SiO_2 system, and their intrinsic luminescence was attributed to Bi^{3+} centers [44]. At the same time, the doping of sillenite-composition glasses with lanthanide ions has not been described so far. The closest analogues are compounds of the eulytine structure: $Bi_4Si_3O_{12}$:Er, Yb crystals (σ_{em} = 0.98×10^{-20} cm^2, τ = 8.46 ms, bandwidth 16 nm) [45], $Bi_4Si_3O_{12}$:Er^{3+} glass [46], and a $Bi_4Si_3O_{12}$:Er^{3+} crystal under laser diode excitation [47], as well as Er: $Bi_4(Ge_{0.5}Si_{0.5})_3O_{12}$ with σ_{em} = 2.25×10^{-20} cm^2 and τ = 5.19 ms [48]. To the best of our knowledge, the luminescence of Er^{3+} and Yb^{3+} ions in glass of the sillenite composition $Bi_{12}SiO_{20}$ (Bi_2O_3:SiO_2 = 6:1), i.e., with a Bi_2O_3 content far exceeding the range covered in [19], has not been studied so far. Compared with other oxide materials, the sillenite host has a high refractive index and a low phonon energy, which reduces the probability of non-radiative transitions. This is particularly important for devices operating in the IR spectral region, where the energies of radiative transitions are small.

The aim of this work is to study the structure, elemental composition, and luminescent properties of sillenite-type $Bi_{12}SiO_{20}$ glass doped with ytterbium and erbium ions, and to elucidate the mechanism of excitation energy transfer between the impurity ions by measuring the absorption, luminescence excitation, near-infrared photoluminescence, and upconversion luminescence spectra. A mechanism of excitation energy transfer from Yb^{3+} to Er^{3+} ions upon resonant absorption of 980 nm radiation is proposed. Notably, the intense intracenter emission of Er^{3+} ions in the 1.5 μm region has a bandwidth and cross-section that make this glass an active medium for broadband amplification in the C+L bands of fiber-optic communication links.

2. Experimental details

2.1. Synthesis

$Bi_{12}SiO_{20}$:Yb,Er glass was prepared in two stages. First, polycrystalline bismuth silicate $Bi_{12}SiO_{20}$ was prepared by solid-state synthesis: a stoichiometric mixture of the starting reagents, prepared according to the reaction $6Bi_2O_3 + SiO_2 \rightarrow Bi_{12}SiO_{20}$, was placed in a ceramic crucible and heated at T = 600 °C for 6 hours, then cooled to room temperature. The product was then thoroughly ground in an agate mortar to a fine powder. High-purity bismuth oxide Bi_2O_3 and silicon oxide SiO_2 (Sigma-Aldrich) were used for the synthesis. Doping with Yb and Er was carried out by adding the appropriate amounts of Yb_2O_3 and

Er_2O_3 to the as-prepared polycrystalline $Bi_{12}SiO_{20}$. Two samples with different lanthanide concentrations were synthesized, hereinafter referred to as BSO-1 (sample 1) and BSO-2 (sample 2). The mixture was ground, placed in an alundum crucible, and melted at T = 1110 °C. The melt was homogenized for two hours, rapidly cooled to ~400 °C, and then cooled inertially in the furnace to room temperature. The synthesized glass is transparent with a yellow tint. For further studies, samples of ~10×8×1.5 mm^3 were cut from the obtained glass, and their surfaces were mechanically ground and polished. Their elemental composition was determined by energy-dispersive spectroscopy (EDS); the results are presented in Table 1.

Table 1. Elemental composition of $Bi_{12}SiO_{20}$:Yb,Er glass according to EDS mapping (at.%).

Sample / area	O	Si	Bi	Al	Yb	Er	Bi/Si
Sample 1 (BSO-1), area 1	75.73	11.18	8.96	4.06	0.07	<0.01	0.80
Sample 1 (BSO-1), area 2	79.11	11.52	9.30	–	0.08	<0.01	0.81
Sample 2 (BSO-2)	77.96	11.62	10.39	–	0.03	<0.01	0.89

2.2. Study of the structure and composition of the samples

The amorphous state of the samples was verified by X-ray diffraction, and the morphology and elemental composition were examined by scanning electron microscopy with energy-dispersive X-ray microanalysis. X-ray diffraction patterns were recorded on a Malvern Panalytical X-ray diffractometer with CuKα radiation in the range 2θ = 5–110°. The surface morphology was studied using a TESCAN VEGA3 scanning electron microscope (accelerating voltage 20 kV, secondary (SE) and backscattered (BSE) electron detectors), and the elemental composition was determined by energy-dispersive X-ray microanalysis (EDS) in mapping mode over areas of ~50–300 μm, with the spectrum averaged over the map area.

2.3. Measurements of absorption and photoluminescence spectra

Absorption spectra in the 435–1050 nm range were measured at room temperature using a setup based on a 60 cm focal length monochromator and a quartz halogen lamp. Luminescence excitation spectra at 1540 nm were recorded in the 300–1000 nm range under excitation with monochromatized radiation from a halogen lamp. Luminescence spectra under laser excitation at λ = 980 nm (Yb laser, P up to 3 W) were measured at room temperature using a 60 cm focal length monochromator and a photomultiplier tube, and in the 1540 nm region using a germanium photodiode. In addition, absorption spectra were recorded with a StellarNet BLUE-Wave spectrophotometer in the 300–1100 nm range in the radiation power measurement mode. These measurements enabled estimation of the quantum yield of upconversion luminescence in the visible range under laser excitation at λ_{ex} = 980 nm.

3. Results and discussion

3.1. Structure, morphology, and elemental composition of the glass

The short-range structure of $Bi_{12}SiO_{20}$ glass consists of a framework of [BiO_5] polyhedra, with the lone electron pair of the Bi^{3+} ion, in whose cavities [SiO_4] tetrahedra are located. Upon doping, trivalent lanthanide ions substitute for Bi^{3+} ions at the low-symmetry site, as shown for Eu^{3+} ions in [42]. Fig. 1 shows the diffraction pattern of the synthesized glass together with that of crystalline $Bi_{12}SiO_{20}$. The pattern contains no Bragg reflections, only

two broad halos with maxima at $2\theta \approx 27.5°$ and $2\theta \approx 43°$, confirming the sample's amorphous state. Notably, both halos coincide with the most intense reflections of crystalline sillenite $Bi_{12}SiO_{20}$ ($2\theta \approx 27.7°$ and 42.9°). This indicates that the glass retains sillenite-type short-range order, i.e., the framework of $[BiO_5]$ polyhedra with $[SiO_4]$ tetrahedra, whereas long-range order is lost. The loss of long-range order leads to a distribution of Er^{3+} ions over sites with different local environments, resulting in inhomogeneous broadening of the f–f transition bands [6].

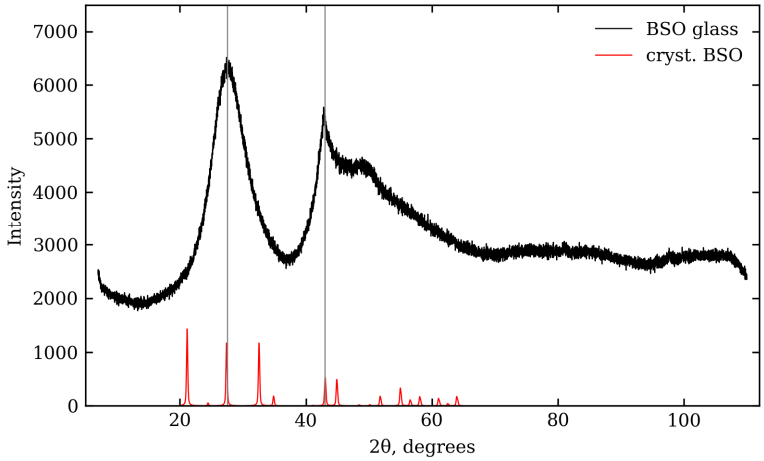


Fig. 1. Diffraction pattern of $Bi_{12}SiO_{20}$:Yb,Er glass (black curve) and of crystalline $Bi_{12}SiO_{20}$ (red).

Fig. 2 shows images of the fracture surface of $Bi_{12}SiO_{20}$:Yb,Er glass obtained in the secondary and backscattered electron modes. The glass is homogeneous over the imaged area: in the BSE image, whose contrast is determined by the mean atomic number, no inclusions, regions of different composition, or signs of phase separation were detected; only the conchoidal fracture and cleavage lines characteristic of glass are observed on the surface. This is consistent with the absence of Bragg reflections in the diffraction pattern (Fig. 1) and indicates that sillenite crystallization does not occur under the chosen melt cooling regime. The results of EDS analysis averaged over the map areas are given in Table 1. Ytterbium ions are distributed uniformly throughout the volume, and their content in sample 1 (0.07–0.08 at.%) is approximately 2–2.5 times higher than in sample 2 (0.03 at.%), which is consistent with the ratio of the Yb^{3+} absorption band intensities in these samples (see Section 3.2). The erbium content is below the detection limit of the EDS method. It should be noted that 4–7 at.% of

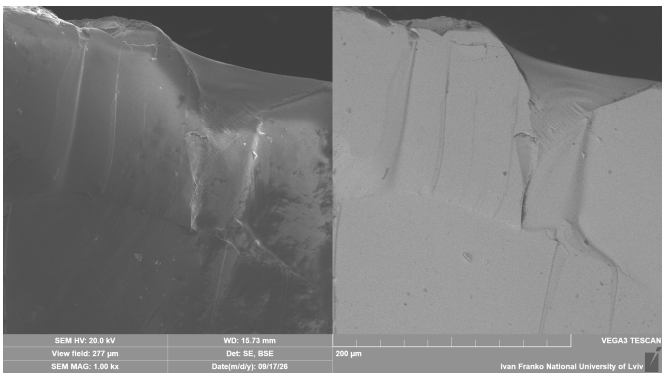


Fig. 2. SEM images of the fracture surface of $Bi_{12}SiO_{20}$:Yb, Er glass in secondary (left) and backscattered (right) electron modes; accelerating voltage: 20 kV; field of view: 277 µm.

aluminum was detected in some areas of the samples; it is natural to assume that it enters the melt as a result of partial dissolution of the alundum crucible material at T = 1110°C. The Al_2O_3 admixture in bismuth silicate glasses is known to stabilize the glassy state, so its presence is not an obstacle to obtaining homogeneous glass, but it may affect the local environment of the impurity ions.

3.2. Absorption and luminescence excitation spectra

Fig. 3 shows the absorption spectra of two samples of $Bi_{12}SiO_{20}$:Yb,Er glass at room temperature over 435–1050 nm. The spectra exhibit bands caused by electronic transitions in Er^{3+} ions from the ground level $^4I_{15/2}$ to the levels $^4F_{7/2}$ (488 nm), $^2H_{11/2}$ (521 nm), $^4S_{3/2}$ (544 nm), $^4F_{9/2}$ (652 nm) and $^4I_{9/2}$ (799 nm), as well as an intense band peaking at 976.5 nm due to the $^2F_{7/2}\rightarrow{}^2F_{5/2}$ transition in Yb^{3+} ions, which overlaps with the $^4I_{15/2}\rightarrow{}^4I_{11/2}$ transition of Er^{3+} ions. On the short-wavelength side of the 976.5 nm band, a broad shoulder is observed in the 900–940 nm region, caused by transitions to the upper Stark components of the $^2F_{5/2}$ level of the Yb^{3+} ion. The bands were identified on the basis of the energy level scheme of the Er^{3+} ion and the results of [45–47]. The most intense Er^{3+} band is the hypersensitive $^4I_{15/2}\rightarrow{}^2H_{11/2}$ band (521 nm), whose intensity is governed by the Ω_2 parameter and is sensitive to local-environment asymmetry and Er–O bond covalency [5]. The high intensity of this band is consistent with the ion's low-symmetry environment at the Bi^{3+} site [42]. Attention should be paid to the fact that the ratio of the intensity of the Yb^{3+} band (976.5 nm) to that of the Er^{3+} band (521 nm) for sample 1 is approximately 1.5 times larger than for sample 2, which reflects the different ratio of ytterbium and erbium concentrations in the samples. The non-selective optical density background (2.3–2.5), which increases towards shorter wavelengths, is due to the fundamental absorption edge and photoionization absorption. For nano-sillenite glass-ceramics, optical band gap values of 2.19–3.24 eV depending on composition were reported in [44]. The strong absorption at 976.5 nm corresponds to the $^2F_{5/2}\rightarrow{}^2F_{7/2}$ electronic transition in Yb^{3+} ions, which determines their role as a sensitizer [33]. For comparison, σ_{abs}(976 nm) = 6.96×10^{-20} cm^2 was obtained in [45] for a $Bi_4Si_3O_{12}$:Er, Yb crystal. For our BSO-1 glass, σ_{abs}(976) = 6.62×10^{-20} cm^2. We previously observed an analogous resonant excitation-energy transfer process from Yb^{3+} ions to Er^{3+} ions in $CsPbCl_3$:Yb,Er perovskite crystals [48].

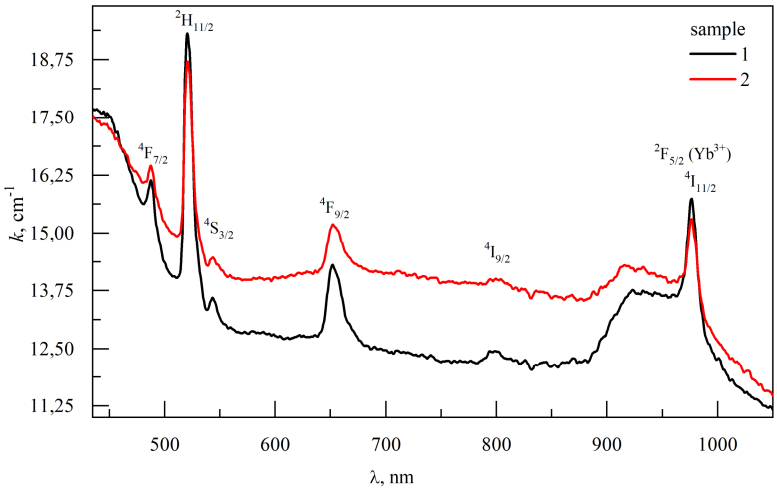


Fig. 3. Absorption spectra of samples 1 and 2 of $Bi_{12}SiO_{20}$:Yb,Er glass at T = 293 K with assignment of the bands to transitions of Er^{3+} and Yb^{3+} ions.

Fig. 4 shows the luminescence excitation spectra of Er^{3+} ions at the wavelength λ_{em} = 1540 nm ($^4I_{13/2}\rightarrow{}^4I_{15/2}$ transition) for samples BSO-1 and BSO-2 at room temperature. The excitation spectra contain all the intracenter absorption bands of Er^{3+} ions recorded in the absorption spectrum (Fig. 3): $^2H_{9/2}$ (408 nm), $^4F_{7/2}$ (490 nm), $^2H_{11/2}$ (523 nm), $^4S_{3/2}$ (544 nm), $^4F_{9/2}$ (655 nm), $^4I_{9/2}$ (794–807 nm), as well as the intense $^2F_{7/2}\rightarrow{}^2F_{5/2}$ band of Yb^{3+} ions (976 nm) with a broad short-wavelength shoulder in the 900–940 nm region. The presence of all Er^{3+} bands in the excitation spectrum indicates that electrons excited to any upper level of the Er^{3+} ion relax, through a cascade of non-radiative transitions, to the metastable $^4I_{13/2}$ level, from which emission in the 1.5 μm region occurs. Notably, the Yb^{3+} band at 976 nm is one of the most intense in the excitation spectrum and is comparable in intensity to the $^2H_{11/2}$ and $^4F_{9/2}$ bands of Er^{3+} ions. Since the Yb^{3+} ion has only one excited level, $^2F_{5/2}$, this is direct evidence of resonant excitation energy transfer from Yb^{3+} to Er^{3+} ions ($^2F_{5/2}\rightarrow{}^4I_{11/2}$) followed by $^4I_{11/2}\rightarrow{}^4I_{13/2}$ relaxation, as occurs in Er/Yb-doped bismuth glasses [23, 35]. The different relative intensity of the Yb^{3+} band in the excitation spectra of samples BSO-1 and BSO-2 is consistent with the different Yb/Er ratio established from the absorption spectra. Note also that a broad band is observed in the 380–430 nm region of the excitation spectrum of sample BSO-1, which, besides the $^4I_{15/2}\rightarrow{}^2H_{9/2}$ transition, may be related to host absorption near the fundamental absorption edge followed by excitation energy transfer to Er^{3+} ions.

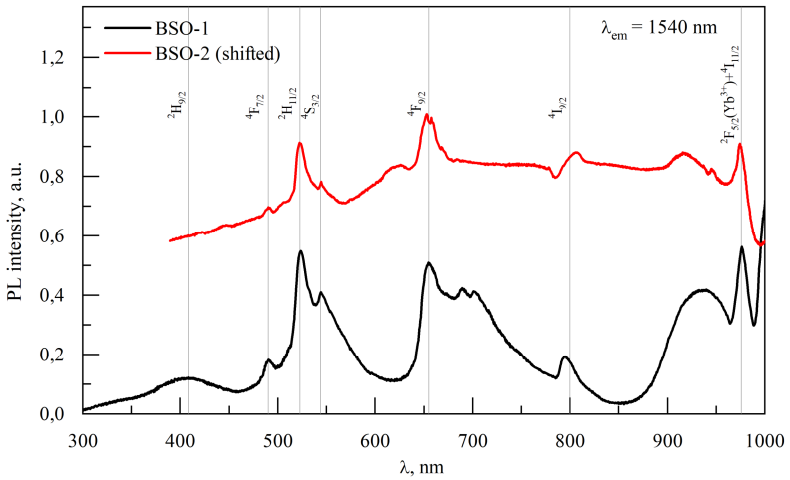


Fig. 4. Luminescence excitation spectra of Er^{3+} ions (λ_{em} = 1540 nm) in BSO-1 and BSO-2 $Bi_{12}SiO_{20}$:Yb,Er glass samples at T = 293 K; the BSO-2 spectrum is shifted along the ordinate axis.

3.3. Luminescence of Er^{3+} ions in the 1.5 μm region

Fig. 5 shows the luminescence spectra of $Bi_{12}SiO_{20}$:Yb,Er glass samples in the near-IR region, excited by Yb laser radiation (λ = 980 nm) at room temperature. The spectrum clearly exhibits an intense asymmetric emission band peaking at 1532 nm, caused by electronic transitions in Er^{3+} ions from the $^4I_{13/2}$ level to the ground level $^4I_{15/2}$. The full width at half maximum (FWHM) is 48 nm for both samples, and at 0.1 of the maximum, the band extends from 1465 to 1600 nm, covering the S-, C-, and L-bands of telecommunication fibers. On the long-wavelength side, the band has a shoulder in the 1560–1600 nm region, caused by transitions from the lower Stark components of the $^4I_{13/2}$ level to the upper components of the $^4I_{15/2}$ level. The obtained bandwidth exceeds the value of 42 nm for binary Bi_2O_3–SiO_2

glass with a Bi_2O_3 content of up to 55 mol.% [19] and is comparable to 45 nm in lead-bismuth halogermanates [25], but is inferior to 65–82 nm in bismuth borosilicate [20, 21] and 52–80 nm in bismuth germanate glasses with WO_3 additions [22], where the broadening is achieved by introducing additional glass formers. At the same time, the bandwidth in the glass is three times larger than the 16 nm in the $Bi_4Si_3O_{12}$:Er, Yb crystal [45], which directly reflects the inhomogeneous broadening of the f–f transitions in a disordered host [6]. It is reasonable to assume that the high Bi_2O_3 content in the sillenite composition provides many non-equivalent sites for Er^{3+} ions in the [BiO_5] polyhedron network, which is the decisive factor in band broadening in bismuthate glasses [11, 12], see Table 2.

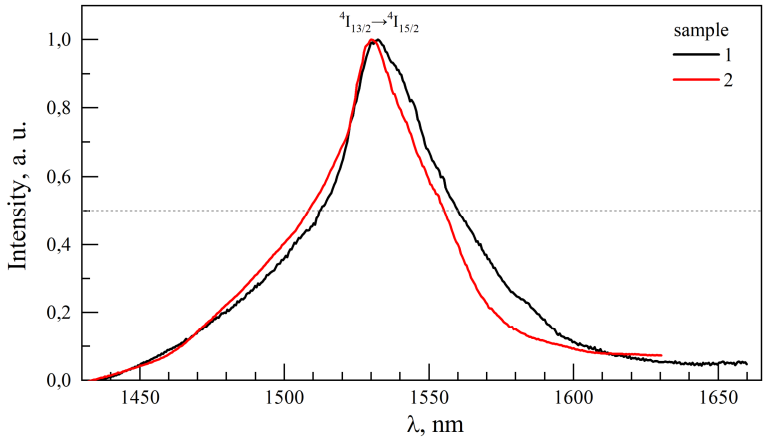


Fig. 5. Normalized photoluminescence spectra of samples 1 and 2 of $Bi_{12}SiO_{20}$:Yb,Er glass in the $^4I_{13}/_2\rightarrow{}^4I_{15}/_2$ transition region of Er^{3+} ions, excited at λ = 980 nm, T = 293 K; the dashed line indicates the half-maximum level.

Table 2. Parameters of the $^4I_{13}/_2\rightarrow{}^4I_{15}/_2$ emission band of Er^{3+} ions in $Bi_{12}SiO_{20}$:Yb, Er glass in comparison with other bismuth-containing hosts.

Host	λ_{max}, nm	$\Delta\lambda$, nm	σ_{em}, 10^{-20} cm^2	$\tau(^4I_{13}/_2)$, ms	Ref.
$Bi_{12}SiO_{20}$:Yb, Er glass (this work)	1532	48	–	–	–
Bi_2O_3–SiO_2 glass (35 mol.% Bi_2O_3)	~1532	42	0.74	5.5	[19]
Bi_2O_3–B_2O_3–SiO_2:Ce, Yb, Er glass	~1535	≈80	0.07–0.25	0.66–0.86	[21]
GeO_2–Bi_2O_3–WO_3:Er glass	~1535	52–80	0.74–0.77	3.6–4.1	[22]
PbO–Bi_2O_3–Ga_2O_3–GeO_2:Er, Yb glass	1532	≈45	0.89	3.41	[25]
Bi_2O_3–B_2O_3:Er glass	~1535	76–86	0.70–0.86	0.5–1.1	[27]
ZnO–Bi_2O_3–B_2O_3:Er, Yb glass	~1532	≈82	0.11–0.73	3.6–4.0	[28]
TeO_2–Bi_2O_3–B_2O_3–ZnO:Er glass	~1535	72	0.91	3.52	[32]
$Bi_4Si_3O_{12}$:Er, Yb crystal	1543	16	0.98	8.46	[45]
$Bi_4(Ge_{0,5}Si_{0,5})_3O_{12}$:Er	~1535	43	2.25	5.19	[49]

3.4. Upconversion luminescence and the mechanism of excitation energy transfer

Under excitation with λ = 980 nm, in addition to the intracenter emission in the IR region, upconversion luminescence of Er^{3+} ions in the visible spectral region is clearly observed in the glass (Fig. 6). The spectrum exhibits radiative transitions to the ground $^4I_{15}/_2$ level from the following excited levels: $^2H_{11}/_2$ (526–532 nm), $^4S_3/_2$ (546 nm), $^4F_9/_2$ (657–658 nm) and $^4I_9/_2$ (780–796 nm, weak band). The green and red bands have a pronounced Stark structure; in particular, the $^4S_3/_2 \rightarrow {}^4I_{15}/_2$ band consists of components at 546 and 552 nm, and the red $^4F_9/_2 \rightarrow {}^4I_{15}/_2$ band consists of components at 657 and 670 nm. The quantum yield of emission in the 1.5 μm region was determined using a photometric sphere and amounts to 10%. At the same time, the quantum yield of upconversion luminescence for both samples is 0.02%. Attention should be paid to the fact that the ratio of the integrated intensities of the red and green bands differs substantially for the two samples: it is 0.66 for sample 1 and 1.10 for sample 2, i.e., in sample 2 the red upconversion luminescence is dominant. Since sample 2 is characterized by a lower relative ytterbium content (Fig. 3), this difference can be explained by the fact that at a lower Yb^{3+} concentration the role of the channel populating the $^4F_9/_2$ level via the $^4I_{13}/_2$ level (cross-relaxation and energy transfer $^4I_{13}/_2 + {}^2F_5/_2 \rightarrow {}^4F_9/_2$) increases, whereas at a higher Yb^{3+} content the sequential two-step population of the $^4F_7/_2 \rightarrow {}^2H_{11}/_2$, $^4S_3/_2$ levels prevails [36].

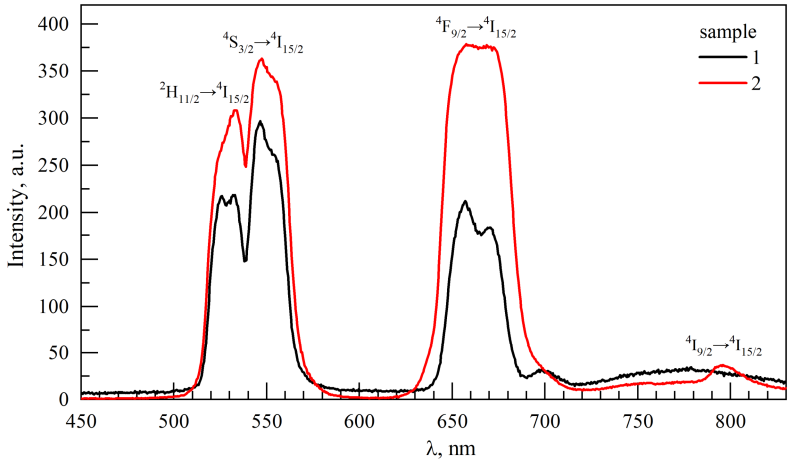


Fig. 6. Upconversion luminescence spectra of samples 1 and 2 of $Bi_{12}SiO_{20}$:Yb, Er glass under excitation with an ytterbium laser, λ = 980 nm, at room temperature.

Upon absorption of ytterbium laser radiation quanta with λ = 980 nm, resonant excitation of Yb^{3+} ions ($^2F_7/_2 \rightarrow {}^2F_5/_2$) and Er^{3+} ions ($^4I_{15}/_2 \rightarrow {}^4I_{11}/_2$) takes place. At the same time, as shown in [33, 35] and as follows directly from the excitation spectra (Fig. 4), resonant excitation energy transfer from the Yb^{3+} ion to the Er^{3+} ion is possible. We assume a two-step energy transfer mechanism (Fig. 7): the first quantum absorbed by the Yb^{3+} ion is transferred to the $^4I_{11}/_2$ level of the Er^{3+} ion (ET_1), and the second one promotes the electron from the $^4I_{11}/_2$ level to the $^4F_7/_2$ level (ET_2), from which the thermally coupled $^2H_{11}/_2$ and $^4S_3/_2$ levels are populated by non-radiative relaxation. The red emission is formed via the $^4I_{13}/_2$ level, populated as a result of $^4I_{11}/_2 \rightarrow {}^4I_{13}/_2$ relaxation, and the subsequent $^4I_{13}/_2 \rightarrow {}^4F_9/_2$ energy transfer [42]. This process is possible because the lifetime of the Er^{3+} ion in the $^4I_{11}/_2$ and $^4I_{13}/_2$ excited states considerably exceeds the photon absorption time of

the Yb^{3+} ion, and in bismuthate hosts the $^4I_{11}/_2$ level lifetime is particularly long (up to 2.45 ms [26]), which favors upconversion. A similar structure of the upconversion spectrum was observed in Er/Yb-doped lead-bismuth halogermanates [25], whereas in binary bismuth borates the upconversion was weak because of the high phonon energy [27]. The relatively intense upconversion in the studied glass is consistent with the low phonon energy of the sillenite host, in which the maximum Bi–O vibration frequencies do not exceed ~600 cm^{-1}, as is known for crystalline sillenites. From the point of view of using the glass as a gain medium, upconversion is a loss channel that takes away part of the population inversion of the $^4I_{13}/_2$ level and of the pump power [14, 15, 34]. Its contribution can be reduced by optimizing the Yb/Er concentration ratio, as well as by co-doping with La_2O_3/B_2O_3, which reduces erbium clustering [14], or with Ce^{3+} ions, which accelerate the $^4I_{11}/_2 \rightarrow {}^4I_{13}/_2$ relaxation and suppress upconversion in bismuth borosilicates [21]. At the same time, the intense visible upconversion luminescence indicates efficient excitation-energy transfer from Yb^{3+} to Er^{3+} ions, a necessary condition for operation of an amplifier pumped at 980 nm.

Shortly, the main results obtained in the present work are as follows: (i) the broad emission band ($\Delta\lambda$ = 48 nm FWHM, ~140 nm at the 0.1 level); (ii) the $^4I_{13}/_2 \rightarrow {}^4I_{15}/_2$ emission band peaking at 1532 nm; (iii) the efficient absorption of 980 nm pump radiation by Yb^{3+} ions; and (iv) the $Yb^{3+} \rightarrow Er^{3+}$ energy transfer confirmed by the excitation spectra. This places $Bi_{12}SiO_{20}$:Yb, Er glass on a par with Bi_2O_3–SiO_2 [19], bismuth borosilicate [20, 21] and bismuth germanate [22, 23] hosts, on the basis of which Bi-EDF amplifiers with a gain bandwidth of 80 nm have been developed [50, 51]. The high Bi_2O_3 concentration and, accordingly, the high refractive index enable compact active elements a few centimeters long [3, 52], as well as planar waveguide amplifiers, for which the large cross-section and high activator solubility are decisive [53]. Modern integrated erbium amplifiers already provide over 30 dB of gain on a chip [2]. For practical use, it is additionally necessary to determine the lifetime of the $^4I_{13}/_2$ level, the stimulated emission cross-section and the gain cross-section, to assess the thermal stability of the

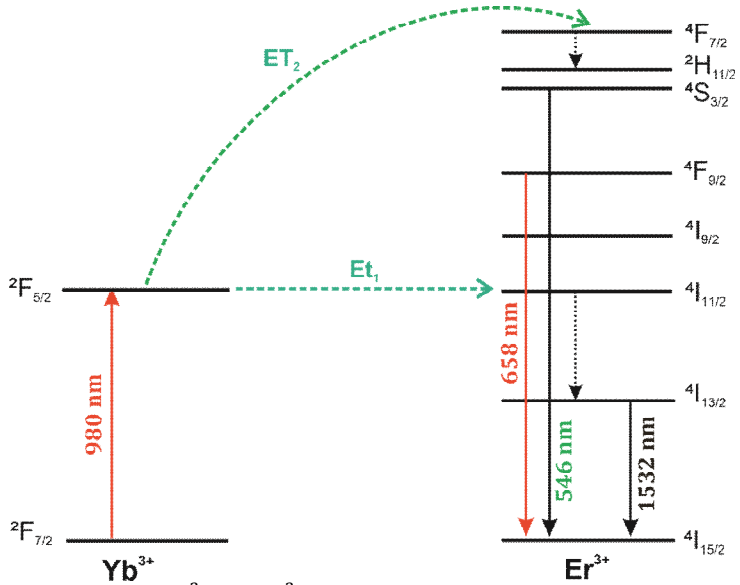


Fig. 7. Energy-level scheme of Yb^{3+} and Er^{3+} ions in $Bi_{12}SiO_{20}$:Yb, Er glass, showing the mechanism of two-step resonant excitation energy transfer (ET_1, ET_2), upconversion, and IR radiative transitions; dashed arrows denote non-radiative relaxation.

glass with regard to fiber drawing or waveguide formation [13], and to minimize the losses associated with upconversion and pair-induced quenching [16, 17], which determine the noise figure of highly doped Bi-EDF [18]. Note also that any phase-insensitive linear amplifier, including an erbium one, is limited by the 3 dB quantum noise limit [54]. Only phase-sensitive schemes can approach or exceed this limit [55]; therefore, the term "quantum amplifier" as applied to an erbium medium should be understood as an amplifier operating close to the quantum noise limit. At the same time, erbium-containing amorphous hosts have already demonstrated their suitability for quantum telecommunication applications, particularly for storing entangled telecom-band photons in erbium-doped fiber [56], which makes broadband erbium-doped bismuth glass of interest in this direction as well.

4. Conclusions

The structure, absorption, excitation, luminescence, and upconversion luminescence spectra of $Bi_{12}SiO_{20}$ glass doped with ytterbium and erbium ions have been studied. It has been established that the glass, synthesized by quenching a melt of nominal composition 92 mol.% $Bi_{12}SiO_{20}$ – 5 mol.% Yb_2O_3 – 3 mol.% Er_2O_3 from T = 1110°C, is nearly homogeneous according to EDS and amorphous according to X-ray diffraction studies, and the positions of the two halos in the diffraction pattern ($2\theta \approx 27.5°$ and 43°) coincide with the most intense reflections of crystalline sillenite, which indicates the retention of sillenite-type short-range order. According to EDS, ytterbium ions are uniformly distributed throughout the volume, and their content in samples 1 and 2 differs by a factor of about 2–2.5. The absorption spectra show the f–f transition bands of Er^{3+} ions and the intense ${}^2F_{7/2} \rightarrow {}^2F_{5/2}$ band of Yb^{3+} ions at 976.5 nm. The luminescence excitation spectra at 1540 nm contain both the bands of Er^{3+} ions and the band of Yb^{3+} ions, providing direct evidence of resonant excitation energy transfer from Yb^{3+} to Er^{3+} ions. Under excitation with λ = 980 nm (Yb laser) at room temperature, intense intracenter emission of Er^{3+} ions in the 1.5 μm region (${}^4I_{13/2} \rightarrow {}^4I_{15/2}$ transition) was recorded, peaking at 1532 nm with FWHM of 48 nm and covering the 1465–1600 nm range at the 0.1 level of the maximum; the bandwidth exceeds the values for binary Bi_2O_3–SiO_2 glasses and $Bi_4Si_3O_{12}$:Er, Yb crystals. Upconversion luminescence of Er^{3+} ions in the green (526–552 nm) and red (657–670 nm) spectral regions was observed, driven by a two-step resonant energy-transfer mechanism from Yb^{3+} to Er^{3+} ions. The ratio of the red and green band intensities (0.66 and 1.10) is determined by the Yb/Er concentration ratio in the samples. Because the sillenite host has low phonon energy, radiative transitions in the IR region are more probable, and the many non-equivalent Er^{3+} sites in the glass provide a broad emission band, making $Bi_{12}SiO_{20}$:Yb, Er glass a promising material for compact broadband C+L-band amplifiers in fiber-optic communication links. Further studies will be aimed at measuring the decay kinetics and transition cross-sections, optimizing the Yb/Er concentration ratio, and directly measuring the gain coefficient.

Funding. The work was partially supported by the Ministry of Education and Science of Ukraine (Grant No. 0125U002198 and Grant No. 0125U002027) and has received funding through the EURIZON project, which is funded by the European Union under grant agreement No.871072.

Disclosures. The authors declare no conflicts of interest.

Authors' contribution. M. Shevchuk-- spectroscopic measurements, writing the manuscript; V. Adamiv - glass synthesis, analysis of the results; I. Teslyuk- analysis of the results; S. Malynych- analysis of the results, writing the manuscript; V. Kordan- analysis of the results; M. Rudysh -

spectroscopic measurements, analysis of the results; T. Demkiv - analysis of the results, writing the manuscript; R. Gamernyk - spectroscopic measurements, analysis of the results, writing the manuscript, supervision.

References

1. Donodin, A., London, E., Correia, B., Virgillito, E., Tan, M., Hazarika, P., Phillips, I., Harper, P., Turitsyn, S. K., Curri, V., & Forysiak, W. (2023). Multi-band ESCL transmission supported by bismuth-doped and Raman fiber amplification. *Journal of Lightwave Technology*, *42* (7), 2317-2327.
2. Liu, Y., Qiu, Z., Ji, X., Lukashchuk, A., He, J., Riemensberger, J., Hafermann, M., Wang, R. N., Liu, J., Ronning, C., & Kippenberg, T. J. (2022). A photonic integrated circuit–based erbium-doped amplifier. *Science*, *376*(6599), 1309–1313.
3. Boetti, N. G., Pugliese, D., Ceci-Ginistrelli, E., Lousteau, J., Janner, D., & Milanese, D. (2017). Highly doped phosphate glass fibers for compact lasers and amplifiers: A review. *Applied Sciences*, *7*(12), 1295.
4. Miniscalco, W. J. (1991). Erbium-doped glasses for fiber amplifiers at 1500 nm. *Journal of Lightwave Technology*, *9*(2), 234–250.
5. Tanabe, S. (2002). Rare-earth-doped glasses for fiber amplifiers in broadband telecommunication. *Comptes Rendus Chimie*, *5*(12), 815–824.
6. Jha, A., Shen, S., & Naftaly, M. (2000). Structural origin of spectral broadening of 1.5-μm emission in Er^{3+}–doped tellurite glasses. *Physical Review B*, *62*(10), 6215–6227.
7. Mori, A., Ohishi, Y., & Sudo, S. (1997). Erbium-doped tellurite glass fibre laser and amplifier. *Electronics Letters*, *33*(10), 863–864.
8. Ohishi, Y., Mori, A., Yamada, M., Ono, H., Nishida, Y., & Oikawa, K. (1998). Gain characteristics of tellurite-based erbium-doped fiber amplifiers for 1.5-μm broadband amplification. *Optics Letters*, *23*(4), 274–276.
9. Mori, A., Kobayashi, K., Yamada, M., Kanamori, T., Oikawa, K., Nishida, Y., & Ohishi, Y. (1998). Low noise broadband tellurite-based Er^{3+}-doped fibre amplifiers. *Electronics Letters*, *34*(9), 887–888.
10. Mori, A., Sakamoto, T., Kobayashi, K., Shikano, K., Oikawa, K., Hoshino, K., Kanamori, T., Ohishi, Y., & Shimizu, M. (2002). 1.58-μm broad-band erbium-doped tellurite fiber amplifier. *Journal of Lightwave Technology*, *20*(5), 822–827.
11. Tanabe, S., Sugimoto, N., Ito, S., & Hanada, T. (2000). Broad-band 1.5 μm emission of Er^{3+} ions in bismuth-based oxide glasses for potential WDM amplifier. *Journal of Luminescence*, *87–89*, 670–672.
12. Sugimoto, N. (2002). Ultrafast optical switches and wavelength division multiplexing (WDM) amplifiers based on bismuth oxide glasses. *Journal of the American Ceramic Society*, *85*(5), 1083–1088.
13. Yang, J., Dai, S., Zhou Y.; Wen L.; Hu L. Jiang Z. (2003). Spectroscopic properties and thermal stability of erbium-doped bismuth-based glass for optical amplifier. *Journal of Applied Physics*, *93*(2), 977–983.
14. Hayashi, H., Ohara, S., Sugimoto, N., & Tanabe, S. (2007). Effects of lanthanum and boron addition on suppression of cooperative upconversion in bismuth oxide-based erbium-doped fibers. *Japanese Journal of Applied Physics*, *46*(6R), 3452–3454.
15. Hayashi, H., Tanabe, S., & Sugimoto, N. (2008). Quantitative analysis of optical power budget of bismuth oxide-based erbium-doped fiber. *Journal of Luminescence*, *128*(3), 333–340.
16. Jung, M.-W., Shin, J.-H., Jhon, Y.-M., & Lee, J.-H. (2010). A theoretical and experimental investigation into pair-induced quenching in bismuth oxide-based erbium-doped fiber amplifiers. *Journal of the Optical Society of Korea*, *14*(4), 298–304.
17. Delevaque, E., Georges, T., Monerie, M., Lamouler, P., & Bayon, J.-F. (1993). Modeling of pair-induced quenching in erbium-doped silicate fibers. *IEEE Photonics Technology Letters*, *5*(1), 73–75.
18. Paul, M. C., Harun, S. W., Huri, N. A. D., Hamzah, A., Das, S., Pal, M., Bhadra, S. K., Ahmad, H., Yoo, S., Kalita, M. P., Boyland, A. J., & Sahu, J. K. (2010). Performance comparison of Zr-based and Bi-based erbium-doped fiber amplifiers. *Optics Letters*, *35*(17), 2882–2884.
19. Yang, J., Dai, S., Dai, N., Xu, S., Wen, L., Hu, L., & Jiang, Z. (2003). Effect of Bi_2O_3 on the spectroscopic properties of erbium-doped bismuth silicate glasses. *Journal of the Optical Society of America B*, *20*(5), 810–815.
20. Wang, X., Nie, Q., Xu, T., Dai, S., Shen, X., & Liu, L. (2007). Optical spectroscopy and energy transfer of Er^{3+}/Ce^{3+} in B_2O_3-doped bismuth-silicate glasses. *Journal of the Optical Society of America B*, *24*(4), 972–978.
21. Chu, Y., Ren, J., Zhang, J., Peng, G., Yang, J., Wang, P., & Yuan, L. (2016). $Ce^{3+}/Yb^{3+}/Er^{3+}$ triply doped bismuth borosilicate glass: A potential fiber material for broadband near-infrared fiber amplifiers. *Scientific Reports*, *6*, 33865.
22. Çamiçi, H. C., Guérineau, T., Rivera, V. A. G., Falci, R. F., LaRochelle, S., & Messaddeq, Y. (2023). The role of tungsten oxide in Er^{3+}-doped bismuth-germanate glasses for optical amplification in L-band. *Scientific Reports*, *13*, 8835.
23. Tan F., XuP., Zhou D., Wang L., Yang Q., Song X., Han K. (2021). 1.53 μm luminescent properties and energy transfer processes of Er^{3+}/Yb^{3+} co-doped bismuth germanate glass laser material. *Journal of Luminescence*, *239*, 118300.
24. Muzyka T. M.; Pushak A. S., Furgala Y. M., Malynych S. Z., Moroz I. E., Kotlov A., Demkiv T. M., Voloshinovskii A. S., & Gamernyk R. V. (2024). Enhancing up-conversion luminescence in Yb/Er co-doped $CsPbCl_3$ sing le crystals. *Journal of Applied Physics*, *136*, 215103.

25. Yang, G. F., Shi, D. M., Zhang, Q. Y., & Jiang, Z. H. (2008). Spectroscopic properties of Er^{3+}/Yb^{3+}-codoped PbO–Bi_2O_3–Ga_2O_3–GeO_2 glasses. *Journal of Fluorescence*, *18*(1), 131–137.
26. Guo, Y., Li, M., Hu, L., & Zhang, J. (2012). Intense 2.7 μm emission and structural origin in Er^{3+}-doped bismuthate (Bi_2O_3–GeO_2–Ga_2O_3–Na_2O) glass. *Optics Letters*, *37*(2), 268–270.
27. Oprea, I.-I., Hesse, H., & Betzler, K. (2006). Luminescence of erbium-doped bismuth–borate glasses. *Optical Materials*, *28*(10), 1136–1142.
28. Hegde, V., Devarajulu, G., Pramod, A. G., Kolavekar, S. B., Aloraini, D. A., Almuqrin, A. H., Sayyed, M. I., & Jagannath, G. (2022). Analysis of optical and near-infrared luminescence of Er^{3+} and Er^{3+}/Yb^{3+} co-doped heavy metal borate glasses for optical amplifier applications. *Photonics*, *9*(5), 355.
29. Musalikunta, P., Nirlakalla, R., Ravanamma, R., Gaddam, N., Kummara, V. K., Bahajjaj, A. A. A., Reddy, N. N. K., & Kagola, U. K. (2025). Optimizing energy transfer in Er^{3+}/Yb^{3+} co-doped heavy metal oxide bismuth borate glasses for C-band optical amplifiers. *Optical Materials*, *163*, 116939.
30. Seema T., Umar S. A., Lakhwant S., Vanita T. (2022). Effect of Er^{3+} ions on the structural, optical and Judd–Ofelt intensity parameters of (Bi_2O_3–$BaTiO_3$) glass system and their application as fiber-amplifier. *Materials Chemistry and Physics*, *262*, 126782.
31. Liu, J., Yin, P., Shao, X., Jiang, Y., & Zhao, G. (2024). Enhancement of near-infrared emission of Er^{3+} in tellurite glasses by reducing the phonon energy with Bi_2O_3 content. *Journal of Materials Science: Materials in Electronics*, *35*, 2285.
32. Tan, F., Xie, G., Ma, Y., Zhang, Y., Gao, B., Cui, S., Chen, D., Ban, Y., & Zhou, D. (2024). Structure and spectral properties of Er^{3+}-doped bismuth telluride near-infrared laser glasses. *Materials*, *17*(13), 3292.
33. Townsend, J. E., Barnes, W. L., Jedrzejewski, K. P., & Grubb, S. G. (1991). Yb^{3+} sensitised Er^{3+} doped silica optical fibre with ultrahigh transfer efficiency and gain. *Electronics Letters*, *27*(21), 1958–1959.
34. Hwang, B.-C., Jiang, S., Luo, T., Watson, J., Sorbello, G., & Peyghambarian, N. (2000). Cooperative upconversion and energy transfer of new high Er^{3+}- and Yb^{3+}–Er^{3+}-doped phosphate glasses. *Journal of the Optical Society of America B*, *17*(5), 833–839.
35. Liu, Y., Chen, Y., Lin, Y., Tan, Q., Luo, Z., & Huang, Y. (2007). Energy transfer in Yb^{3+}–Er^{3+}-codoped bismuth borate glasses. *Journal of the Optical Society of America B*, *24*(5), 1046–1052.
36. Auzel, F. (2004). Upconversion and anti-Stokes processes with f and d ions in solids. *Chemical Reviews*, *104*(1), 139–174.
37. Chen, G., Ohulchanskyy, T. Y., Kachynski, A., Ågren, H., & Prasad, P. N. (2011). Intense visible and near-infrared upconversion photoluminescence in colloidal $LiYF_4$:Er^{3+} nanocrystals under excitation at 1490 nm. *ACS Nano*, *5*(6), 4981–4986.
38. Fujimoto, Y., & Nakatsuka, M. (2001). Infrared luminescence from bismuth-doped silica glass. *Japanese Journal of Applied Physics*, 40(3B), L279–L281.
39. Peng, M., Qiu, J., Chen, D., Meng, X., Yang, I., Jiang, X., & Zhu, C. (2004). Bismuth- and aluminum-codoped germanium oxide glasses for super-broadband optical amplification. *Optics Letters*, *29*(17), 1998–2000.
40. Peng, M., Zhang, N., Wondraczek, L., Qiu, J., Yang, Z., & Zhang, Q. (2011). Ultrabroad NIR luminescence and energy transfer in Bi and Er/Bi co-doped germanate glasses. *Optics Express*, *19*(21), 20799–20807.
41. Luo, Y., Yan, B., Zhang, J., Wen, J., He, J., & Peng, G.-D. (2018). Development of Bi/Er co-doped optical fibers for ultra-broadband photonic applications. *Frontiers of Optoelectronics*, *11*(1), 37–52.
42. Kowalczyk, M., Kaczkan, M., Majchrowski, A., & Malinowski, M. (2023). A comparative study of Eu^{3+}-doped sillenites: $Bi_{12}SiO_{20}$ (BSO) and $Bi_{12}GeO_{20}$ (BGO). *Materials*, *16*(4), 1621.
43. Xu, H., Zhang, Y., Zhang, H., Yu, H., Pan Z., Wang Y., Sun S., Wang J., Boughton R.I. (2012). Growth and characterization of Nd:$Bi_{12}SiO_{20}$ single crystal. *Optics Communications*, *285*(19), 3961–3966.
44. Almasarawi, O. N., Hamzawy, E. M. A., Margha, F. H., Souaya, E. R., & Abdel-Hameed, S. A. M. (2022). Preparation and characterization of a novel luminescence nano-sillenite ($Bi_{12}SiO_{20}$) glass ceramic within Bi_2O_3–ZnO–SiO_2 system. *Applied Physics A*, *128*, 1126.
45. Zhang Y., Hu S., Tian T, Xiao X., Chen Y., Zhang Y., Xu, J. (2022). Growth and spectral properties of Er^{3+} and Yb^{3+} co-doped bismuth silicate single crystal. *Crystals*, *12*(11), 1532.
46. Lira, A. C., Martín-Rodríguez E., Martínez-Martínez R., Camarillo I., Muñoz G.H., Garcia-Solé J., Caldiño U. (2010). Spectroscopy of the $Bi_4Si_3O_{12}$:Er^{3+} glass for optical amplification and laser application. *Optical Materials*, *32*(10), 1266–1273.
47. Lira, C. A., Ramírez M.O., García J.S., Caldiño U. (2007). Photoluminescence of $Bi_4Si_3O_{12}$:Er^{3+} crystal excited in the commercial laser diode emission region. *Optical Materials*, *29*(6), 605–609.
48. T. M. Muzyka, A. S. Pushak, Y. M. Furgala, S. Z. Malynych, I. E. Moroz, A. Kotlov, T. M. Demkiv, A. S. Voloshinovskii, R. V. Gamernyk. Enhancing up-conversion luminescence in Yb/Er co-doped CsPbCl3 single crystals. J. Appl. Phys. *136*, 215103 (8 p.), (2024).
49. Shao, Y., Chen, Y., Ma, Z., Zhang, M., Xu, J., Lu, J., Li, Z., & Zhang, Q. (2022). Synthesis and property investigation of Er-doped $Bi_4(Ge_{0.5}Si_{0.5})_3O_{12}$ (BGSO): A potential gain medium of C-band laser. *Applied Physics A*, *128*, 920.
50. Ohara, S., Sugimoto, N., Ochiai, K., Hayashi, H., Fukasawa, Y., Hirose, T., Nagashima, T., & Reyes, M. (2004). Ultra-wideband amplifiers based on Bi_2O_3-EDFAs. Optical Fiber Technology, *10*(3), 283–295.
51. Sotobayashi, H., Gopinath, J. T., & Ippen, E. P. (2003). 23 cm long Bi_2O_3-based EDFA for picosecond pulse amplification with 80 nm gain bandwidth. Electronics Letters, *39*(19), 1356–1358.

52. Kuroiwa, Y., Sugimoto, N., Ochiai, K., Ohara, S., Fukasawa, Y., Ito, S., Tanabe, S., & Hanada, T. (2001). Fusion spliceable and high efficient Bi_2O_3-based EDF for short-length and broadband application pumped at 1480 nm. Optical Fiber Communication Conference (OFC 2001), paper TuI5.
53. Bradley, J. D. B., & Pollnau, M. (2011). Erbium-doped integrated waveguide amplifiers and lasers. *Laser & Photonics Reviews*, *5*(3), 368–403.
54. Caves, C. M. (1982). Quantum limits on noise in linear amplifiers. *Physical Review D*, *26*(8), 1817–1839.
55. Tong, Z., Lundström, C., Andrekson, P. A., McKinstrie, C. J., Karlsson, M., Blessing, D. J., Tipsuwannakul, E., Puttnam, B. J., Toda, H., & Grüner-Nielsen, L. (2011). Towards ultrasensitive optical links enabled by low-noise phase-sensitive amplifiers. *Nature Photonics*, *5*, 430–436.
56. Saglamyurek, E., Jin, J., Verma, V. B., Shaw, M. D., Marsili, F., Nam, S. W., Oblak, D., & Tittel, W. (2015). Quantum storage of entangled telecom-wavelength photons in an erbium-doped optical fibre. *Nature Photonics*, *9*, 83–87.

Shevchuk, M., Adamiv, V., Teslyuk, I., Malynych, S., Kordan, V., Rudysh, M., Demkiv, T., Gamernyk, R. (2026). Optical Properties and Upconversion Luminescence of $Bi_{12}SiO_{20}$:Yb,Er Glass. *Ukrainian Journal of Physical Optics*, *27*(4), 04193 – 04206.
doi: 10.3116/16091833/Ukr.J.Phys.Opt.2026.04193

Анотація. *У роботі досліджено люмінесценцію скла $Bi_{12}SiO_{20}$, легованого іонами ітербію та ербію за різних співвідношень їхніх концентрацій. Згідно з даними рентгенівської дифракції, скло є аморфним, проте зберігає ближній порядок, характерний для структури типу силеніту. У спектрах поглинання та збудження люмінесценції спостерігаються смуги, що відповідають f–f-переходам іонів Er^{3+}, а також інтенсивна смуга іонів Yb^{3+} (976,5 нм), зумовлена переходом $^2F_{7/2}\rightarrow{}^2F_{5/2}$. Наявність смуги іонів Yb^{3+} у спектрі збудження люмінесценції на довжині хвилі 1540 нм є прямим свідченням резонансного перенесення енергії збудження від іонів Yb^{3+} до іонів Er^{3+}. При збудженні випромінюванням із довжиною хвилі λ = 980 нм спостерігається інтенсивна внутрішньоцентрова люмінесценція іонів Er^{3+} (перехід $^4I_{13/2}\rightarrow{}^4I_{15/2}$), максимум якої припадає на 1532 нм, а повна ширина на рівні половини максимуму становить 48 нм. Крім того, виявлено зелену (526–552 нм) та червону (657–670 нм) ап-конверсійну люмінесценцію, зумовлену двостадійним механізмом перенесення енергії від Yb^{3+} до Er^{3+}. Встановлено, що ширина смуги випромінювання в діапазоні 1,5 мкм перевищує відповідні значення, відомі для бінарних стекол системи Bi_2O_3–SiO_2 та кристалів $Bi_4Si_3O_{12}$:Er,Yb. Це робить скло $Bi_{12}SiO_{20}$:Yb,Er перспективним активним середовищем для широкосмугових оптичних підсилювачів, що працюють у діапазонах C+L.*

Ключові слова: *силеніт $Bi_{12}SiO_{20}$, вісмутове скло, ербій, ітербій, люмінесценція в діапазоні 1,5 мкм, ап-конверсія, оптичний підсилювач*